Total (p, n) reaction cross section study on ^{51}V over the incident energy range 1·56 to 5·53 MeV

M K MEHTA, S KAILAS and K K SEKHARAN*
Nuclear Physics Division, Bhabha Atomic Research Centre, Bombay 400 085
*Cyclotron Institute, Texas A and M University, College Station, Texas, 77843, USA

Abstract. The total (p, n) reaction cross section for ^{51}V has been measured as a function of proton energy in the energy range 1·56 to 5·53 MeV with thick and thin targets. The fluctuations in the fine resolution excitation functions were analysed, to extract $\langle \Gamma \rangle$, the coherence width. The thick target excitation function suitably averaged over appropriate energy intervals has been compared with the optical model, Hauser-Feshbach and Hauser-Feshbach-Moldauer calculations. The strong isobaric analog resonance at $E_p \sim 2\cdot340$ has been shape analysed to extract the proton width Γ_p, the spreading width W and the spectroscopic factor.

1. Introduction

The total (p, n) reaction cross section measurements in medium weight nuclides have contributed significantly to the understanding of nuclear reaction mechanism and nuclear structure. They have yielded information on compound nuclear levels in case of isolated resonances and average compound nuclear widths and strength functions in case of high level densities (Iyengar *et al* 1967; Johnson and Kernell 1970). The identification and location of isobaric analog resonances (IAR) through (p, n) excitation function measurement is a standard practice (Couchell *et al* 1967, Balamuth *et al* 1968, Fox and Robson 1966). When an IAR is much below the Coulomb barrier, the shape analysis of the excitation function measured over the resonance has yielded the relevant parameters with better accuracies than what is possible through elastic scattering studies (Sekharan and Mehta 1972, Sekharan and Mehta 1969, Kailas 1977). Such measurements below the Coulomb barrier have also been used to extract optical model parameters for the target plus proton system (Johnson and Kernell 1970, Albert 1959, Kailas *et al* 1975a). Finally the (p, n) reaction, generally on a light target, is an established means for obtaining monoenergetic neutrons for neutron reaction studies. The reaction ^{51}V(p, n)^{51}Cr is a useful neutron source (Harris *et al* 1962), especially for low energy neutrons as the negligible centre of mass effect in this case does not become a limitation to the lowest energy of the emitted neutrons.

The study of the reaction ^{51}V(p, n)^{51}Cr over the incident energy range starting from near the threshold ($\sim 1\cdot564$ MeV) to the maximum energy available at our

laboratory was undertaken with a view to fulfil all or most of the objectives described above. In section 2, the experimental procedure and the results are discussed. The analysis of the results and extraction of (a) the average level widths through Ericson fluctuation analysis (Ericson 1963), (b) the strength function SFN, (c) the optical model parameters and (d) the parameters for the observed IAR both through the Robson theory (Robson 1965) and Breit Wigner analysis are described in section 3. The conclusions are discussed in section 4.

2. Experimental procedure and results

2.1. *Thick and thin target excitation functions*

The ^{51}V targets were prepared by evaporating natural vanadium metal (^{51}V abundance 99.76%) on to thick tantalum or aluminium foils. Analysed proton beam from the 5·5 MeV Van de Graaff accelerator at our laboratory was collimated on the target which itself served as a Faraday cup and was situated at the centre of a 4π geometry neutron counter (Sekharan 1965). The number of incident protons was measured by a *current integrator* (Gupta 1968) with an error of $\pm 1\%$.

The (p,n) excitation function was first measured for the incident energy range 1·9 to 5·5 MeV utilising a thick target (648 μgms/cm^2, $\triangle E \sim 45$ keV for 2 MeV proton) in steps of about 40 keV. This target was made by evaporating vanadium metal on an accurately weighed aluminium foil which was thick enough to stop the protons up to 5·5 MeV. The target thickness was determined by weighing the foil after the target was deposited with an error of $\pm 7\%$. The efficiency of the neutron counter was determined through the measurement of the ^{7}Li$(p,n)^{7}$Be reaction (Sekharan
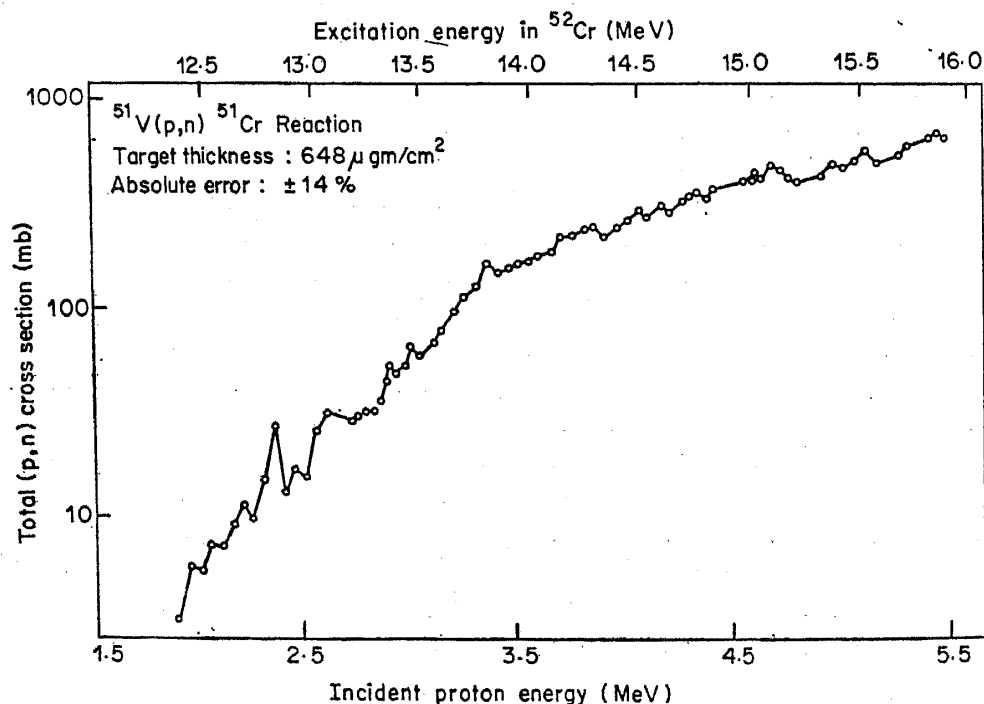

Figure 1. Excitation function for ^{51}V$(p,n)^{51}$Cr reaction using a thick ^{51}V target.

1965), the cross section for which is known with an error of $\pm 5\%$ (Gibbons and Macklin 1959). The measured yield was converted to cross section using standard methods. The resulting excitation function is shown in figure 1. The total absolute error on the cross section is $\pm 14\%$.

The excitation function was remeasured with a thin target (~ 2 keV for 2 MeV protons) in the energy range from 1·56 to 5·53 MeV with an energy step of about 6 keV at lower energies and about 10 keV at higher energy. The results are shown in figures 2 and 3 where only the relative yield has been plotted as a function of bombard-
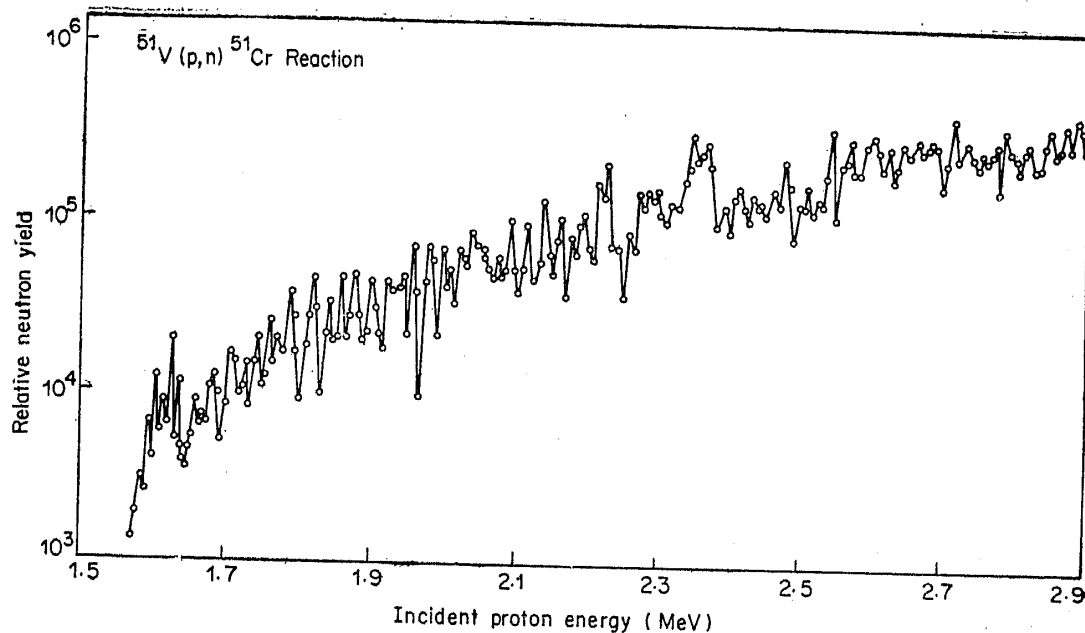

Figure 2. Relative neutron yield for $^{51}V(p,n)^{51}Cr$ reaction (~ 5keV thick target) for E_p range 1·56 to 2·9 MeV.

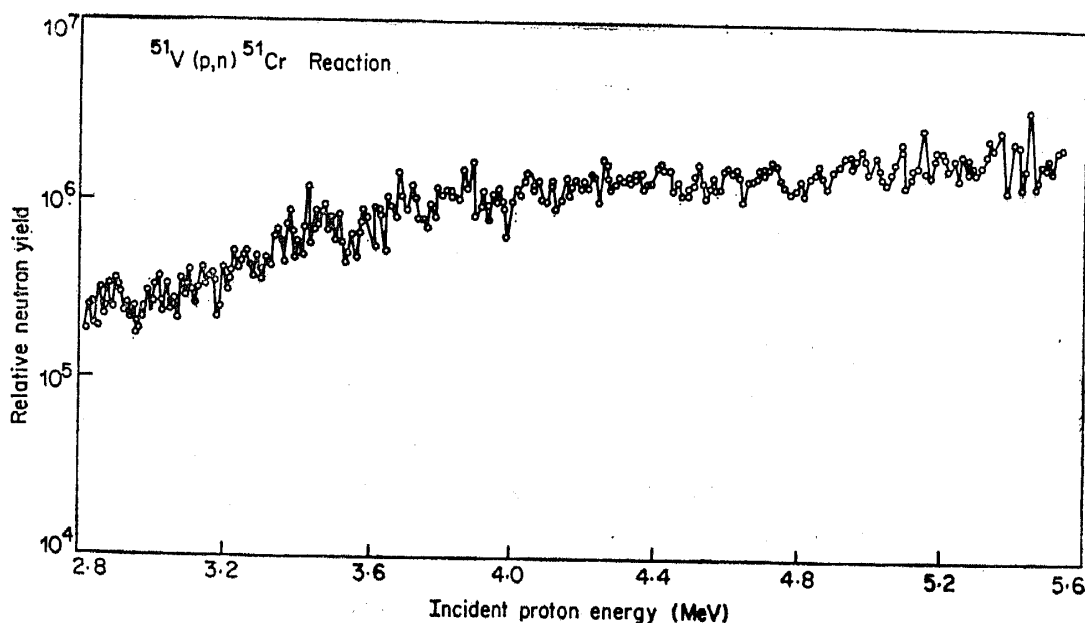**Figure 3.** Relative neutron yield for $^{51}V(p,n)^{51}Cr$ reaction (~ 5 keV thick target) for E_p range 2·8 to 5·53 MeV.

ing energy. This fine excitation function when averaged over 50 keV, closely reproduced the thick target results shown in figure 1.

2.2. *Fine resolution excitation function in the region of the IAR*

A strong, relatively narrow, peak at about 2·4 MeV is the most outstanding feature of the excitation function in figure 1. A large number of IARs have been identified around this region by previous workers (Teranishi and Furbayashi 1966) through γ rays and neutron yield measurement following bombardment of ^{51}V targets by protons. They have also reported a strong IAR around 2·4 MeV bombarding energy. In order to study this region in detail, the neutron yield measurement was repeated in the bombarding energy range from 2·20 to 2·50 MeV with a thinner target ($\sim$1 keV) in steps of 2·5 keV. This excitation function is shown in figure 4. The most spectacular feature is the strong resonance at 2·338 MeV along with two or three weaker peaks at other energies. Although the weaker peaks could be correlated to the IARs identified by Teranishi and Furbayashi (1966) they are too weak to attempt any shape study on them. The level in the compound nucleus ^{52}Cr corresponding to the strong peak at 2·338 MeV has been identified as the isobaric analog of the 1·56 MeV level in the parent nucleus ^{52}V. (Teranishi and Furbayashi 1966, Egan *et al* 1972). The shape analysis of the peak carried out by Teranishi and Furbayashi (1966) as well as an elastic scattering study (Egan 1969) yielded a positive value of the asymmetry parameter $\triangle$ defined in Robson's theory (Robson 1965). If this positive value is correct, it would be hard to justify on theoretical grounds (Robson 1965) and would be contrary to all the measurement of IARs made so far. With a view to determine the shape of the peak more accurately the excitation function was measured over the resonance in steps of 1 keV utilising the thin target. Three independent passes were made over the resonance, the results are shown in
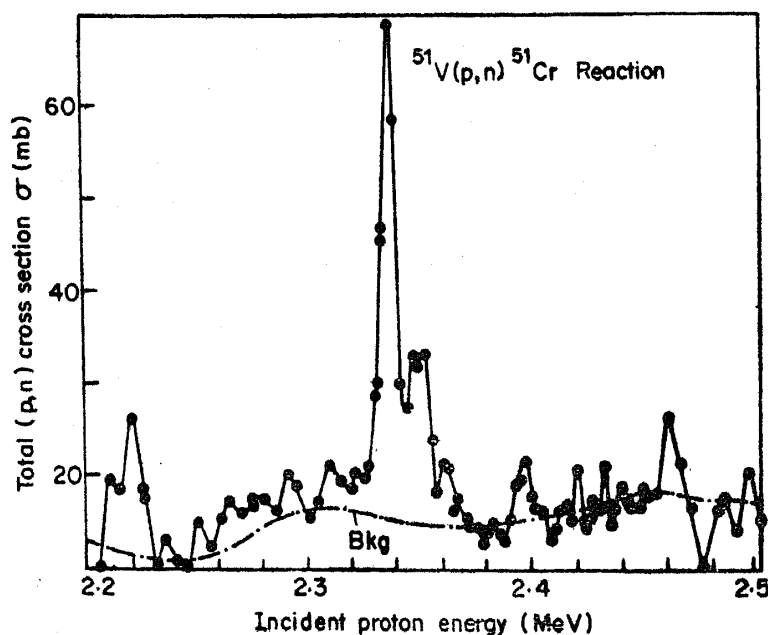
Figure 4. The excitation function for $^{51}V(p, n)^{51}Cr$ reaction in the neighbourhood of the strong IAR at 2·34 MeV. The dash dot line labelled bkg represents the thick target measurement from which the resonance contribution is excluded.
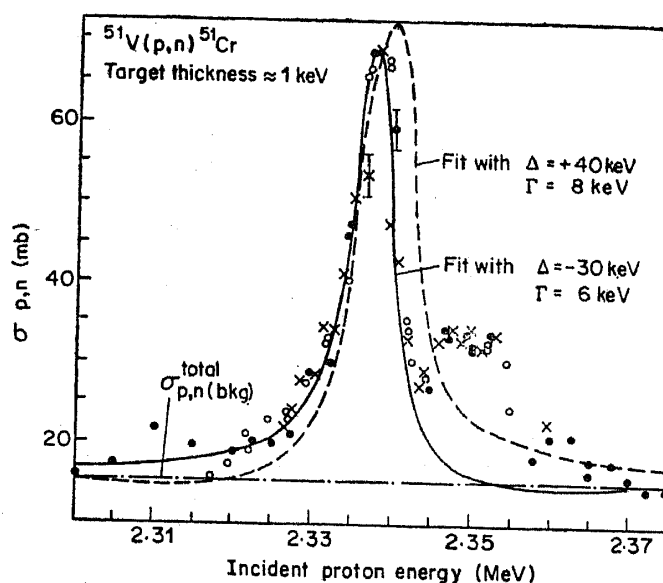
Figure 5. Shape of the IAR at 2·34 MeV measured in 1 keV steps. The solid line is a fit calculated with the negative $\triangle$ and dashed line with positive $\triangle$. The crosses, the open circles and solid dots represent three separate runs over the resonance.

figure 5, where the three separate data sets are indicated by the open circles, filled in circles and the crosses respectively. The thickness for this target was determined by the measurement of elastically scattered alpha particle yield from this target at 2 and 3 MeV bombarding energies at forward angles and fitting the Rutherford cross section expression to the angular distributions. The target thickness was found to be 16 ± 1 μgms/cm^2 ($\sim$1 keV for 2 MeV protons). An overall absolute error of 13% and a relative error of 7% were estimated for the results shown in figure 5 in which the relative error is indicated by error bars on a few data points. Counting statistics error was negligible.

3. Analysis

3.1. *Fluctuations*

For the incident energy range 2·55 to 5·53 MeV in this experiment the compound nucleus ^{52}Cr would be excited to an energy range of about 13 to 16 MeV. For a medium weight nucleus like ^{52}Cr at this high excitation energy the statistical assumption of completely overlapping levels would be valid. The excitation functions in this region exhibit a large number of sharp and overlapping structures which seem to be damped out as the energy increases (figures 2 and 3). This, along with the expected continuum condition for the level density (the ratio of the average level width Γ to average level separation D, is much greater than unity i.e. $\Gamma/D \gg 1$), indicated that interpretation of the fine structure in terms of Ericson fluctuations is justified. (Ericson 1963, Brink and Stephen 1963, and Ericson and Mayer Kuckuk 1966). Thus the excitation functions in this region were subjected to the standard fluctuation analysis (Ericson and Mayer Kuckuk 1966). The region below 2·50 MeV, although containing sharp structure, is known to be modulated by the presence of a number of

IARs (Teranishi and Furbayashi 1966) and hence was left out of this analysis. The parameter of importance in case of the overlapping levels is the average width Γ which can be identified with the coherence width extractable from an autocorrelation analysis of the observed fluctuations. The autocorrelation function $C(\varepsilon)$ is defined as (Mehta *et al* 1966)

$$C(\varepsilon) = \left(\frac{\triangle E}{E_2 - E_1}\right) \sum_{E=E_1}^{E_2} \left(\frac{\sigma(E)}{\langle \sigma(E) \rangle_\delta} - 1\right)\left(\frac{\sigma(E+\varepsilon)}{\langle \sigma(E+\varepsilon) \rangle_\delta} - 1\right) \qquad (1)$$

E_2, E_1 are the upper and lower limits of the bombarding energy, $\sigma(E)$ is the cross section at the bombarding energy E corresponding to each data point on the excitation function, $\triangle E$ is the energy step with which the excitation function is measured, the symbol $\langle \rangle_\delta$ indicates the average cross section over an energy range δ and ε is the energy increment equal to $n \times \triangle E$ with n as an integer.

As the energy step $\triangle E$ was not uniform throughout the whole range of bombarding energy the excitation function was divided into two ranges; 2·545 to 3·84 MeV and 3·84 to 5·53 MeV. The energy step could be assumed to be uniform but different over each of these two parts. Using the expression given above the value of the correlation functions were calculated for the two ranges (designated as $C_1(\varepsilon)$ and $C_2(\varepsilon)$ respectively) for various values of the energy averaging interval δ. The importance of choosing the right value for δ for correlation analysis in presence of gross modulation has been discussed by Mehta *et al* (1966). Following the procedure described in that reference the values of $C_1(0)$ and $C_2(0)$ are plotted as a function of δ in figure 6. It can be observed that $C_1(0)$ and $C_2(0)$ both rise initially for small values of δ and remain more or less constant for a range of values of δ. As discussed by Mehta *et al* (1966), to extract the coherence width from the correlation function the value of δ should be chosen from the flat portion of the curves of figure 6.

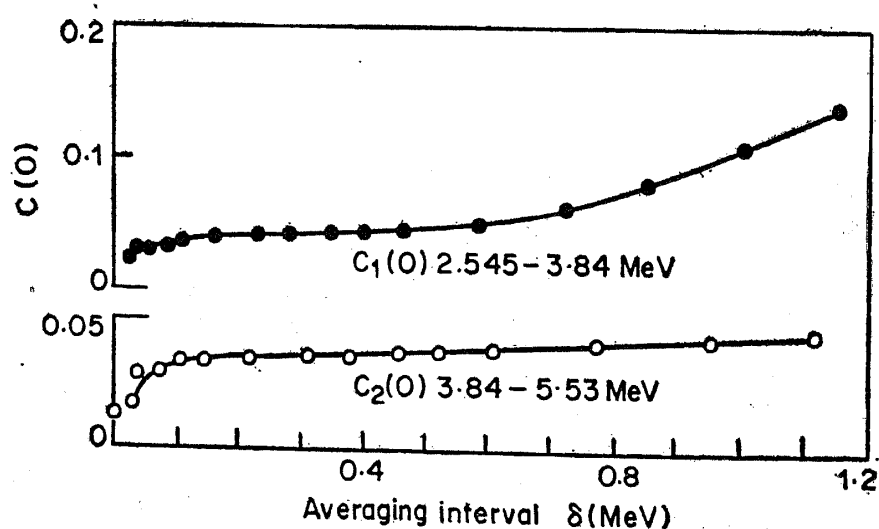**Figure 6.** Autocorrelation function $C(O)$ is plotted as a function of averaging interval δ separately for the energy ranges $E_p = 2 \cdot 545$ to 3.84 MeV (denoted as $C_1('O')$) and $E_p = 3 \cdot 84$ to 5.53 MeV (denoted as $C_2(O)$.)

According to the fluctuation theory (Ericson and Mayer Kuckuk 1966) for small values of ε, $C(\varepsilon)$ is given by

$$C(\varepsilon) = C(0) \frac{\Gamma^2}{\Gamma^2 + \varepsilon^2}. \tag{2}$$

In figure 7, $C_1(\varepsilon)$ for $\delta = 287$ and 345 keV and $C_2(\varepsilon)$ for $\delta = 304$ and 378 keV are plotted as a function of ε. The solid lines are the Lorentzian curves given by expression 2 above. As the Lorentzian shape is expected only for the very low values of ε and since the energy step is large compared to the coherence width Γ, only first few points lie on the curves. The values of Γ for each fit is indicated on the corres-
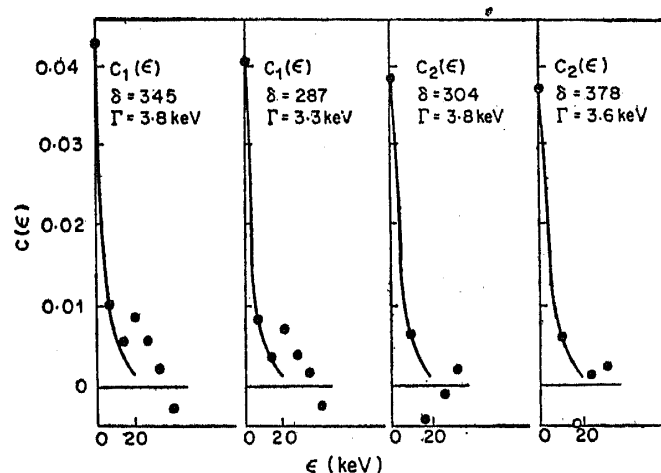

Figure 7. Autocorrelation function $C(\varepsilon)$ is plotted as a function of ε (the energy increment) for four different values of δ. The crosses are the experimental values of $C(\varepsilon)$ for various values of ε. The continuous lines are the Lorentzian fit to the same taking only the first 2 or 3 points.
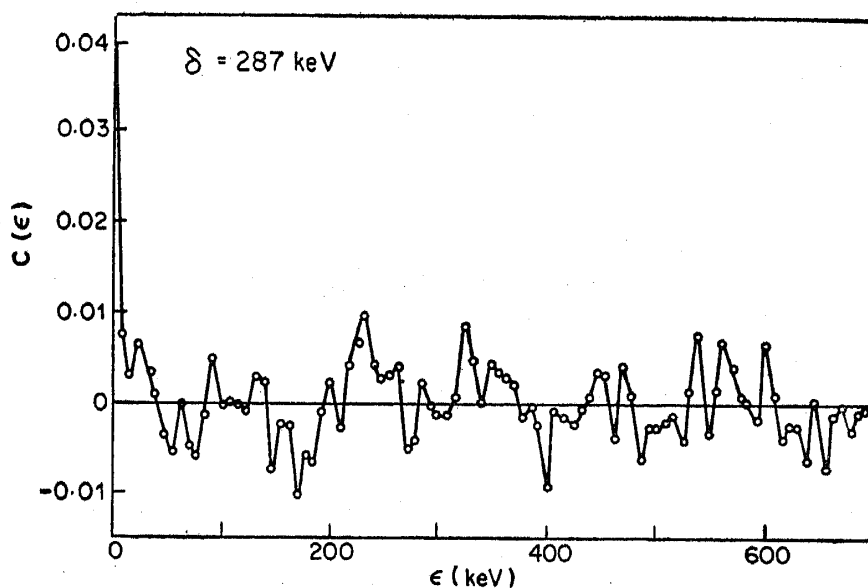

Figure 8. Autocorrelation function $C(\varepsilon)$ is shown as a function of ε for $\delta = 287$ keV. For large values of ε, the $C(\varepsilon)$ fluctuates about $C(\varepsilon)=0$.

ponding figure. Since only two or three points lie on the curves the extracted value of Γ could have large error.

For larger values of ε the $C(\varepsilon)$ values are expected to fluctuate strongly about the value zero due to the finite size sample effects (Ericson and Mayer Kuckuk 1966). The beginning of such fluctuations are seen in figure 7 and can be seen over a larger range of ε in figure 8, where $C(\varepsilon)$ with the δ value of 287 keV is plotted over a larger range of ε. The value of Γ obtained for the several δ values taken from the flat portion of figure ranged from 3·3 to 3·8 keV for both $C_1(\varepsilon)$ and $C_2(\varepsilon)$. Considering the difference in the Γ value obtained by fitting expression (2) to the first and the second points or the first and the third points of the $C(\varepsilon)$ versus ε plot, respectively, together with the variations of Γ with δ and the finite range data error called FRD error (Gibbs 1965), the average level width Γ determined through this analysis can be quoted as $3 \cdot 5 \begin{smallmatrix} +0 \cdot 5 \\ -1 \cdot 3 \end{smallmatrix}$ keV. This compares well with the value of $4 \pm 0·8$ keV obtained from a $^{51}V(p, p)^{51}V$ reaction study (Lamba *et al* 1968, Sood 1968).

3.2. *Strength function*

Another quantity of interest in case of high compound nuclear level densities is the strength function (SFN) (Johnson and Kernell 1970, Kailas *et al* 1975a) which is defined as $\langle \gamma^2 \rangle / D$. $\langle \gamma^2 \rangle$ is the average reduced width for levels with a particular value of the quantum numbers J and π, and D is the average spacing of these levels. The SFN reflects the contribution to the cross section that comes from the nuclear structure aspects of the compound nucleus as the effect of the kinematic factors like Coulomb barrier penetration and angular momentum on the observed excitation function are removed by defining the SFN in this manner (Schiffer and Lee 1958, Margolis and Weisskopf 1957, Johnson and Kernell 1970). Following the procedure described by Johnson and Kernell (1970) the average proton strength function was calculated from the thick target excitation function shown in figure 1, and was found to be $0·37 \pm 0·07$ fm. The error indicated reflects the variation of SFN over the energy range covered in the excitation function. This value along with similar SFN measured for targets with mass numbers between 45 to 59 has yielded some evidence for the presence of a D wave size resonance (Kailas 1977) expected in this mass region (Schiffer and Lee 1958).

3.3. *Optical model analysis*

For a compound nuclear process the reaction cross section is given by the Hauser-Feshbach expression (HF) based on the statistical model (Hauser and Feshbach 1952) and when level width fluctuations are taken into account the cross section is given by Moldauer (1964). When the proton transmission coefficient can be neglected in comparison with the neutron transmission coefficients the HF and HFM expressions reduce to a simple one which is the same as that obtained for the total reaction cross section in the optical model (Kailas *et al* 1975a). This condition is well satisfied for bombarding energies below the Coulomb barrier which is $\sim$6 MeV (for $R_0 = 1·2$ fm) in the present case. Thus it would be meaningful to fit the measured excitation function (suitably averaged to smooth out the small amount of structure) with the optical model prediction of the total reaction cross section and extract the relevant optical model parameters for the target plus proton system.

Optical model calculations were carried out with the optical model code Abacus II (Auerbach 1962) starting with parameters similar to Egan *et al* (1970). As the total reaction cross section would be most sensitive to the value of the imaginary potential V_I, the computer programme was used to search for the best value of V_I keeping all the other parameters fixed. The minimum χ^2 criterion was used to get the best fit. This fit is shown in figure 9 along with the potential parameters used. HF and HFM calculations were also done using the computer code HAFEC (Kailas *et al* 1976) and the fits are also shown in figure 9. The values of the proton and neutron parameters used in these calculations are also indicated in the figure. In the present case the optical model, HF and HFM give equally good fits to the data within the experimental error. For the fits shown in figure 9, the proton optical parameters were adjusted (keeping neutron optical parameters same as that of Egan *et al* 1970) to get the best fit for HF and HFM calculations. It can be seen that the total reaction cross section predicted by this set of proton parameters is very close to the (*p, n*) reaction cross section value obtained through HF calculation. This would justify an attempt discussed earlier to search for a set of proton optical parameters, which would yield the total reaction cross section to fit the present data. This was attempted and the best fit is shown in figure 10. The excellent fit verifies that the condition mentioned above ($\sigma_{p,n} \approx \sigma_R$) is satisfied and the determination of the optical parameters for such sub Coulomb energies through fittings the (*p, n*) cross section data to total reaction cross section predicted by the optical model is justified. It should be mentioned that the more conventional method of determining optical model parameters through the angular distributions measurements for the elastic scattering cross section would not be suitable at these sub Coulomb energies as the forward angle scattering would
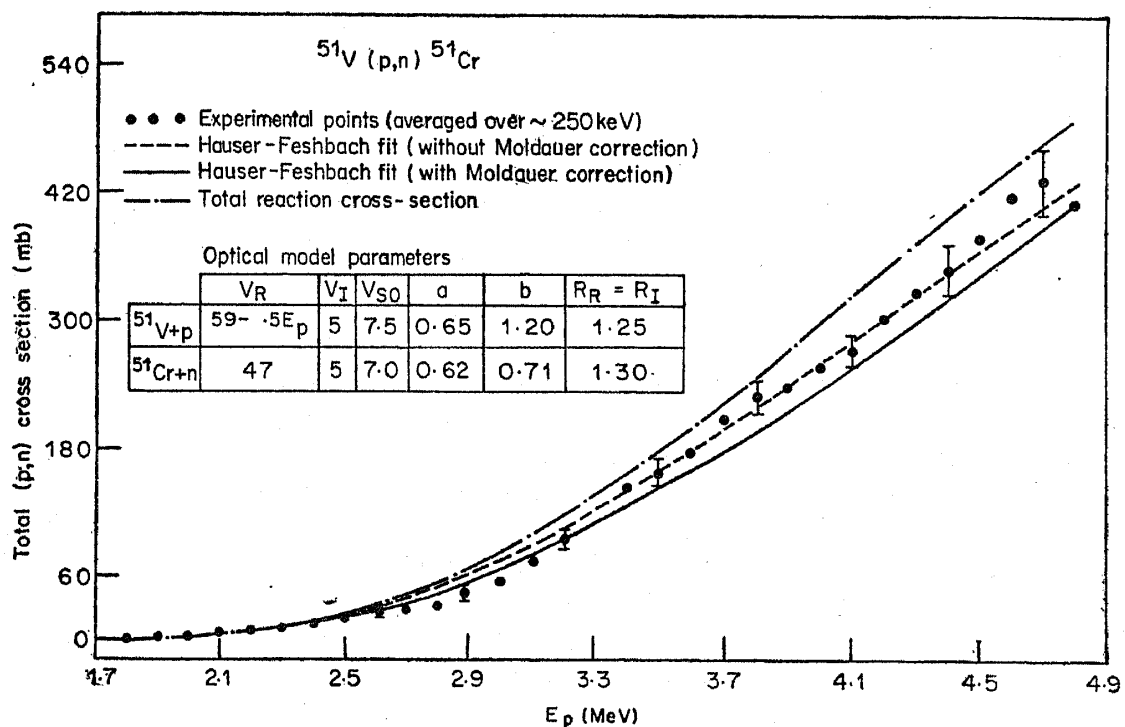

^{51}V (p,n) ^{51}Cr

● ● ● Experimental points (averaged over ~250 keV)
– – – – Hauser-Feshbach fit (without Moldauer correction)
——— Hauser-Feshbach fit (with Moldauer correction)
—·—·— Total reaction cross-section

Optical model parameters

	V_R	V_I	V_{SO}	a	b	$R_R = R_I$
$^{51}V+p$	59– ·5E_p	5	7·5	0·65	1·20	1·25
$^{51}Cr+n$	47	5	7·0	0·62	0·71	1·30·

Figure 9. Optical model, HF and HFM fits to $^{51}V(p, n)^{51}Cr$ data averaged over large energy interval (~100 keV). The optical model parameters used are listed in the figure.
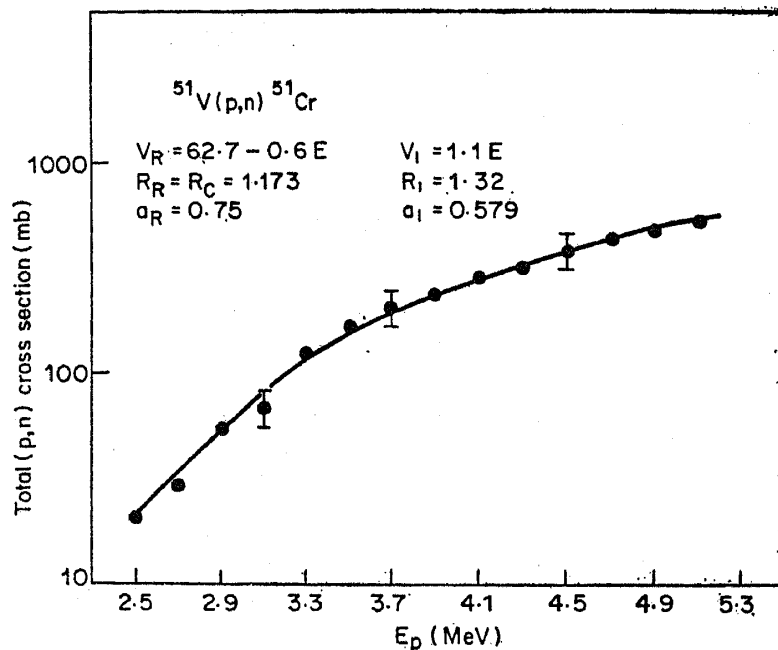
Figure 10. The best optical model (σ_R) fit to $^{51}V(p,n)^{51}Cr$ data. Both V_R and V_I are varied to fit the data. (Derivative Woods-Saxon form factor for V_I).

be dominated by the Coulomb scattering and at backward angles contribution from compound elastic process may be comparable to the potential scattering. A preliminary report of a more exhaustive optical model analysis of (p, n) reaction data at sub Coulomb energies on targets in the mass number range 45-49 carried out at this laboratory has been published elsewhere (Kailas *et al* 1975b).

3.4. *Isobaric analog resonance at 2·338 MeV*

3.4a. *General remarks and useful expressions:* As mentioned earlier the strong resonance seen at 2·338 MeV in figure 4 has been identified as an isobaric analog resonance formed by $l=1$ proton leading to a 4^+ level in the compound nucleus ^{52}Cr at 12·8 MeV excitation which is the analog of the 1·56 MeV level in the parent nucleus ^{52}V. The detailed fine resolution excitation function shown in figure 5 resolved the discrepancy regarding the positive value of the parameter reported by Teranishi and Furbayashi (1966) as discussed by Sekharan and Mehta (1972) who also extracted the spectroscopic factor SF from the Breit Wigner analysis of the resonance.

The purpose of the present analysis was to extract the IAR parameters (Kailas and Mehta 1976) through a more rigorous analysis following Robson's theory (Robson 1965), examine the validity of the assumption made in the previous work (Sekharan and Mehta 1972) and to study the effect of the channel parameters on the extracted value of the spectroscopic factor.

The expressions for the IAR observed in a (p, n) reaction are given by Johnson *et al* (1968) based on the Robson's R-matrix formalism. These were used to carry out the present analysis and are reproduced below for the sake of completeness

$$\sigma_{p^*, n} \text{ (res)} = \sigma_{p^*, n} \text{ (bkg)} \left[\frac{(E-E_0+\triangle)^2}{(E-E_0)^2+\Gamma_0^2/4} - 1 \right] \tag{3}$$

where $\sigma_{p*,\,n}$ (bkg) $= g^{J}\pi\,\lambda^{2}\,T_{p}*$ (4)

and E_0, $\triangle$, Γ_0

are the resonance energy, asymmetry parameter and full width at half maximum of the IAR. g^{J} is the usual statistical weight factor given as $(2J+1)/[(2I+1)(2s+1)]$, J=IAR spin, I=target spin, s=projectile spin. $T_{p}*$=non-resonant transmission factor for the same partial wave that would exist if the resonance were absent and can be calculated using the optical model. It is assumed that neutron transmission coefficient T_n is very large compared to proton transmission coefficient T_p. Determining $\triangle$ from the shape analysis of the resonance utilising the expression (3) one can proceed to extract Γ_p, the proton partial width using the expression,

$$\frac{2\triangle}{\Gamma_p} = -\frac{(S_{p}*-B_c)}{P_{p}*}$$ (5)

where $S_{p}*$, B_c and $P_{p}*$ are the shift factor, boundary condition parameter and penetrability respectively, using R-matrix terminology. Knowing Γ_p, the spreading width W may be extracted from the equation

$$W. = \pi\,s_{p}*\,(S_{p}*-B_c)^2\,\frac{\Gamma_p}{P_{p}*}$$ (6)

where $s_{p}*$ is the proton strength function. At sub Coulomb energies the expression (3) reduces to the conventional Breit-Wigner formula for an isolated resonance as has been shown by Jones (1966). Thus an analysis based on the Breit-Wigner formula also should result in equivalent values for Γ_p and Γ_n, the latter is identified with W of the present analysis.

3.4b. *Extraction of* $\triangle$, Γ_0, Γ_p *and* W: The excitation function shown in figure 5 clearly indicates the presence of a second peak around 2·35 MeV. Therefore, before fitting the resonance shape with expression (3), the contribution to the cross section due to the second peak in the region of the IAR was substracted out by reflecting the higher energy side shape of the second peak to the lower energy side. The resultant pure IAR shape was then fitted by the expression (3). To calculate the quantity σ_p (bkg), the off resonance cross section, the HF calculation (Kailas *et al* 1973) as discussed in section 3.3, with the known level schemes of ^{51}V and ^{51}Cr (Lederer *et al* 1968, Egan *et al* 1972) has been performed. The transmission factor T_p obtained in this fitting was used to calculate $\sigma_{p*,\,n}$ (bkg) from the expression (4). The HF fit yielded a value of $T_{p}*$ (T_p for l=1 protons) to be $4·6\times10^{-3}$ and the corresponding value of $\sigma_{p*,\,n}$ (bkg)$\sim$0·7 mb. A non-linear least squares computer programme has been used to fit expression (3) to the data with E_0, $\triangle$, Γ_0 as free parameters. The experimentally measured IAR corrected for the higher level contribution and the theoretical fit to the data with E_0=2·338 MeV, Γ_0=5·87 keV, $\triangle$=$-$24 keV are shown in figure 11. The $\triangle$ and Γ_0 obtained from the present work are in fair agreement with the earlier results of Sekharan and Mehta (1972).

Having extracted $\triangle$ one can proceed to extract Γ_p and W utilising the expressions (5) and (6). For the present case, $S_{p}*$ is the p wave (l_p=1) proton shift factor and
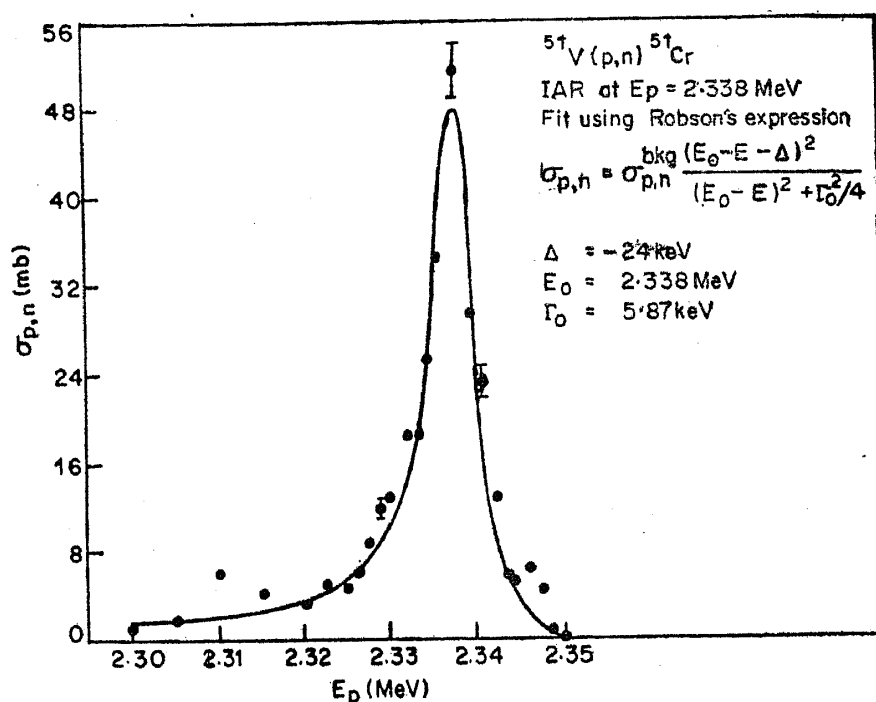
Figure 11. The Robson-Johnson shape fit to the IAR after subtraction of the contribution from the higher resonance.

B_c the boundary condition parameter has been equated to the shift factor in the $|nA\rangle$ channel as per normal practice where $|nA\rangle$ implies the channel in which neutron emission occurs to the isospin analog of the ^{51}V ground state. This is a negative energy channel since the Q value for (p, n) reaction between the isobaric analog and the ground states is negative and numerically equal to the Coulomb displacement energy 8·139 MeV while the proton energy is only 2·34 MeV, which is less than the threshold for the $|nA\rangle$ channel. The value of l_n is also taken as unity.

The difficulty with this type of R matrix analysis is the dependence of S_{p*}, B_c and P_{p*} on the channel radius value. This in turn leads to the dependence of Γ_p and hence W on matching radius. In order to study this dependence detailed calculations of Γ_p and W for various values of channel radii have been performed, over the physically meaningful range. A plot of Γ_p and W as a function of matching radius R_0 is shown in figure 12. The minimum or maximum value of Γ_p and W as the case may be, are taken as the optimum Γ_p and W values. The values were $\Gamma_p\sim$ 0·58 keV and $W\sim$4·6 keV and $\Gamma_p+W\sim$5·2 keV. No errors are indicated on these numbers because of their channel parameter dependence as discussed above. [However, if one takes the optimum Γ_p and W values (minimum or maximum as the case may be) the error introduced in their extraction from Robson analysis is of the order of 7%]. In the previous Breit-Wigner analysis of this resonance (Sekharan and Mehta 1972), out of the two numbers extracted for partial widths (5·4 and 0·6 keV), the *larger* number was associated with Γ_p and the smaller number with Γ_n. This was an ad hoc assumption. The present rigorous analysis yields results equivalent to this earlier work as expected (see discussion in section 3.4a). However, the identification of Γ_p and Γ_n is wrong in the earlier work. The present value of $\Gamma_p\sim$0·6 keV is the same as the *smaller* of the two partial widths and $W\sim$4·6 keV of the present analysis is comparable to the larger of the two partial widths extracted
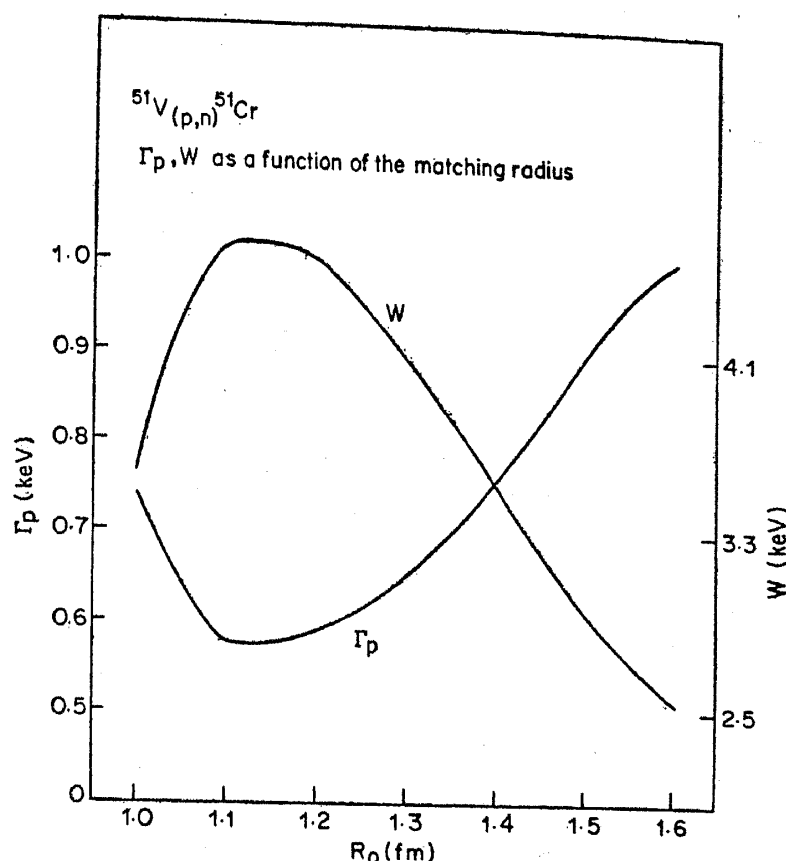
Figure 12. The variation of Γ_p and W as a function of the matching radius R_0.

from the earlier Breit-Wigner analysis. A theoretical estimate for the value of Γ_p for the present case has been made by Pal and Krishan (1976) who find that value lies in the range of 0·8 to 2·2 keV. The present result of $\Gamma_p \sim 0·6$ keV is comparable to the lower limit of this range, especially considering the channel radius dependence of the Γ_p value.

It should be noted that the sum of Γ_p and W, i.e. $\Gamma_p + W = 5·2$ keV, which is expected to be equal to Γ_0, the total width extracted from the shape of the resonance. However the value of Γ_0 is found to be 5·87 keV and is thus slightly larger than the sum of Γ_p and W. This may be expected in the (p, n) measurement (Robson 1969).

3.4 c. *Spectroscopic factor*

The important nuclear structure quantity " spectroscopic factor " extracted from an IAR analysis is expected to be the same as the one extracted from (d, p) data on the same target for the parent level (Thompson and Ellis 1969). In cases when (d, p) spectroscopic factors are not measured this is the only way to extract this significant quantity. The proton width Γ_p is related to the proton reduced width through the relation $\Gamma_p = 2 P \gamma_p^2$ where P is the penetrability and γ_p^2 is the reduced proton width. Then utilising the expression $\gamma_p^2 = \gamma_n^2/(2T_0 + 1)$ ($T_0 =$ isospin of target) connecting proton and neutron reduced width as given by Robson (1965), γ_n^2 can be determined. The spectroscopic factor SF is given by $SF = \gamma_n^2/\gamma_{sn}^2$ where γ_{sn}^2 is the single particle reduced width. Utilising the expressions given by Thompson *et al* (1968), and the computer code SSEARCH (Van Bree 1975), SF was calculated

as a function of the channel radius starting from the value of Γ_p determined in the present case. The usual practice is to choose the minimum value of SF where the variation with channel radius is minimum (Thompson *et al* 1968). Further as the bound state neutron wave function itself changes depending on the neutron potentials and parameters used, the SF calculated for the same channel radius will vary with the neutron potential parameters. The SF for various values of the neutron radius parameter is shown in figure 13 along with the proton single particle width Γ_c as a function of R_n. The variation of SF is mainly due to the variation of γ_{sn}^2. It should be noted that for $R_n=1\cdot2$, SF$=0\cdot1$. As the (d, p) work on ^{51}V for neutron populating the parent state is not available in literature, a comparison of SF extracted from the (p, n) reaction in this work with that extracted from (d, p) work cannot be made.

From the above analysis it is clear that the value of SF extracted through such analysis is also sensitive to variation of the opitcal model parameters used in the calculation. In the same way the SF obtained from (d,p) study is also sensitively dependent on the optical model parameters. This parameter dependence of SF has to be taken into account before one considers the comparison of SFs from the two studies. Rapaport and Kerman (1968) and Clarkson *et al* (1971) have suggested procedures to overcome this problem. Following Rapaport and Kerman (1968) who defined the quantity reduced normalisation Λ_c in the (d, p) work as $\Lambda_c=N^2(\text{SF})/k^3$ where N is the normalisation factor obtained from wave function matching and k is the wave number corresponding to neutron binding energy for the state in question, Clarkson *et al* (1971) have defined Λ_c in the IAR case as a dimensionless quantity. Following the latter procedure of Clarkson *et al* (1971) the value of Λ_c was extracted for the present case, which is shown in figure 13 where Λ_c is plotted as a function of R_n, neutron radius parameter. It is clear from the plot that
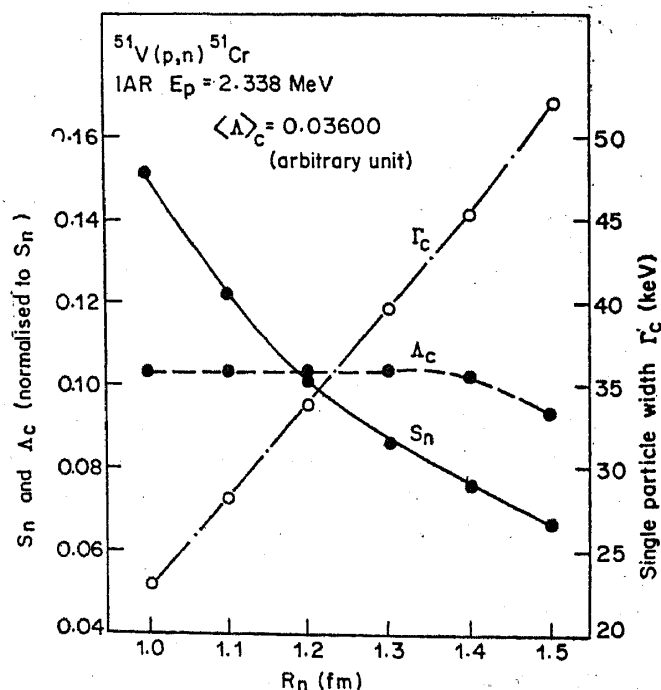

Figure 13. The variation of S_n (neutron spectroscopic factor), Γ_c (proton single particle width) and Λ_c (reduced normalisation) as a function of the neutron radius (R_n) parameter.

Table 1. Summary of the numerical values extracted for the nuclear parameters measured in the work. The optical model parameters refer to the E_p range: 2 to 5 MeV. The Γ and SFN refer to the excitation energy range $\sim 12\cdot5$ to 16 MeV in the compound nucleus ^{52}Cr.

Quantity	Value	
(a) Average compound nuclear width coherence width—Γ	$3\cdot5\,^{+\cdot5}_{-1\cdot3}$ keV	
(b) Strength function SFN	$0\cdot37\pm0\cdot07$ fm	
(c) Optical parameters real potential V_R	$59-0\cdot5\,E_P$	
Imaginary potential V_I (Gaussian form factor)	5	
Radius parameter (real and imaginary) $R_R=R_I$	$1\cdot25$	
Spin orbit potential	$7\cdot5$	
Diffuseness parameter (real potential) a	$0\cdot65$	
Gaussian width (imaginary potential) b	$1\cdot20$	
(d) Isobaric analog resonance (IAR)		
E_0 ————————	$2\cdot338\pm0\cdot001$ MeV	
Γp ————————	$0\cdot58\ \pm0\cdot04$ keV	Robson's
W ————————	$4\cdot6\ \pm0\cdot3$ keV	Method
Γp ————————	$0\cdot6\ \pm0\cdot06$ keV	Breit-Wigner
$\Gamma n(=W)$ ————————	$5\cdot4\ \pm0\cdot6$ keV	Method
$SF(=S_n)$ ————————	$0\cdot1$ at $R_n=1\cdot2$ fm	
Λc ————————	$0\cdot036$ (arbitrary unit)	

Λ_c is relatively insensitive to the variation of R_n as compared to the strong dependence of SF on the above mentioned parameter. The above analysis establishes the usefulness of the quantity Λ_c for comparison with (d, p) work. However, in the present study this type of comparison could not be made as there is no (d, p) work which gives absolute SF for the state in question.

4. Results and conclusions

The present study of (p, n) reaction cross section has resulted in producing numerical values for a number of parameters significant to nuclear reactions as well as nuclear structure studies. These are summarised in table 1.

Acknowledgements

References

Albert R D 1959 *Phys. Rev.* **115** 925
Auerbach E H 1962 BNL-6562
Balamuth D P, Couchell G P and Mitchell G E 1968 *Phys. Rev.* **170** 995
Brink M and Stephen R O 1963 *Phys. Lett.* **5** 77

P.—8

Clarkson R G, Von Brentano P and Harney H L 1971 *Nucl. Phys.* **A161** 49
Couchell G P, Balamuth D P, Horoshko R N and Mitchell G E 1967 *Phys. Rev.* **161** 1147
Egan J J 1969 *Bull. Am. Phys. Soc.* **14** 1216
Egan J J, Dutt G C, McPherson M and Gabbard F 1970 *Phys. Rev.* **C1** 1967
Egan J J *et al* 1972 *Phys. Rev.* **C5** 1562
Ericson T 1963 *Ann. Phys.* **23** 390
Ericson T and Mayer Kuckuk 1966 *Ann. Rev. Nucl. Sci.* **16** 183
Fox J D and Robson D 1966 *Isobaric Spin in Nuclear Physics* (Academic Press)
Gibbons J H and Macklin R L 1959 *Phys. Rev.* **114** 571
Gibbs W R 1965 *Phys. Rev.* **B139** 1185
Gupta S K 1968 *Nucl. Instrum. Methods* **60** 323
Harris K K *et al* 1962 *Bull. Am. Phys. Soc.* **7** 552, 553
Hauser W and Feshbach H 1952 *Phys. Rev.* **87** 366
Iyengar K V K *et al* 1967 *Nucl. Phys.* **A96** 521
Johnson C H, Kernell R L and Ramavatharam S 1968 *Nucl. Phys.* **A107** 21
Johnson C H and Kernell R L 1970 *Phys. Rev.* **C2** 639
Jones G A 1966 *Isobaric Spin in Nuclear Physics* ed. J D Fox and D Robson (Academic Press) 857
Kailas S, Mehta M K and Gupta S K 1973 *Nucl. Phys. Solid State Phys. (India)* **B16** 31
Kailas S *et al* 1975a *Phys. Rev.* **C12** 1789
Kailas S, Mehta M K, Viyogi Y P and Ganguly N K 1975b *Nucl. Phys. Solid State Phys.* (India) **B18** 12
Kailas S, Gupta S K and Mehta M K 1976 BARC I-360
Kailas S and Mehta M K 1976 *Nucl. Phys. Solid State Phys.* (India) **B19** 32
Kailas S 1977 Ph.D. Thesis Bombay University
Lamba C M, Sarma N, Thampi N S and Sood D K 1968 *Nucl. Phys.* **A110** 111
Lederer C M, Hollander J M and Ferlmer I, 1968 *Table of Isotopes* (New York: Wiley)
Margolis E and Weisskopf V F 1957 *Phys. Rev.* **107** 641
Mehta M K, John J, Kerekatte S S and Divatia A S 1966 *Nucl. Phys.* **89** 22
Moldauer P A 1964 *Phys. Rev.* **B135** 642 *Rev. Mod. Phys.* **36** 1079
Pal D and Krishan K 1976 *Nucl. Phys.* **A272** 365
Rapaport J and Kerman A K 1968 *Nucl. Phys.* **A119** 641
Robson D 1965 *Phys. Rev.* **B137** 535
Robson D 1969 *Isospin in Nuclear Physics* ed. D H Wilkinson (North Holland Pub. Co.) 463
Schiffer J P and Lee Jr L L 1958 *Phys. Rev.* **109** 2098
Sekharan K K 1965 M.Sc. Thesis Bombay University
Sekharan K K and Mehta M K 1969 *Proc. Conf. on Properties of Nucl. States*, Montreal 763
Sekharan K K and Mehta M K 1972 *Phys. Rev.* **C6** 2304
Sood D K 1968 Ph.D. (Thesis), IIT, Kanpur
Teranishi E and Furbayashi B 1966 *Isobaric Spin in Nuclear Physics*, ed. J D Fox and D Robson (Academic Press) 640 and *Phys. Lett.* **20** 511
Thompson W J, Adams J L and Robson D 1968 *Phys. Rev.* **173** 975
Thompson W J and Ellis J L 1969 *Nuclear Isopin* ed. J D Anderson *et al* (Academic Press) 689
Van Bree R 1975 (private communication)